High-Resolution Velocity Model Building Using Full Waveform Inversion: A Case Study from Deep-Water Block Mahanadi Basin, India

Saheb Ghosh[1], Deepak Jain[1], Punit Saxena[1], Nikhil Shah[2], Mike Warner[3]*

[1] ONGC, [2] S-Cube, [3] Imperial College London

[*]ghosh_saheb@ongc.co.in

Keywords
Adaptive waveform inversion (AWI), reflection waveform inversion (RWI), least-square waveform inversion (LSFWI), depth interval velocity modelling, depth imaging

Summary

This study demonstrates high-resolution, geologically consistent depth interval velocity model building using full waveform inversion (FWI) applied to narrow-azimuth towed-streamer seismic data from a deep-water block in the Mahanadi Basin, India. We have applied an advanced acoustics anisotropic FWI approach combining adaptive waveform inversion, reflection waveform inversion and least square FWI. Utilization of different type of inversion objective functions prevent the velocity to fall in local-minima and help to achieve viable solution. The final velocity model yields flattened common image gathers, aligns closely with well log velocity trends and demonstrates high trace-to-trace correlation between modelled and observed seismic data. It effectively captures the sedimentary architecture and distinctly delineates the Mio-Pliocene Channel-Levee Complexes (CLCs) which is a proven hydrocarbon-bearing system. This integrated approach delivers a high-resolution velocity model that significantly enhances seismic imaging and supports more accurate hydrocarbon prospect evaluation.

Introduction

High-resolution velocity model building is a critical step in seismic imaging, particularly in deep-water environments where complex subsurface structures and lack of low-frequency signal pose significant challenges. Full waveform inversion (FWI), particularly in its multi-scale implementation (Warner et al., 2013) combining Adaptive Waveform Inversion (AWI), Reflection Waveform Inversion (RWI), and conventional least-square waveform inversion (LS-FWI), has emerged as a powerful tool to address these issues. In this study, we have applied an integrated inversion workflow combining AWI, RWI, and LSFWI for building a high-resolution velocity model in a deep-water block of the Mahanadi Basin, India. The approach draws inspiration from earlier methodological frameworks, such as those proposed by Warner et al., 2016. However, it has been optimized for the geological complexity and data-specific challenges of the study area.

The study area has significant gas accumulation within the CLCs of Miocene-Pliocene sequences. Additionally, the presence of steeply dipping reflectors, complex network of major and minor faults, and Eocene limestone contributes to strong lateral and vertical heterogeneities and pronounced velocity variations. Our integrated AWI-RWI-FWI workflow enables reliable inversion starting from sub-optimal initial models. The use of computationally efficient wave-equation solvers during early iterations accelerates convergence and reduces computational cost (Guasch, L. et al., 2016). This approach ultimately produces a high-resolution, geologically plausible velocity model for seismic imaging and quantitative interpretation.

Underlying Geology

The Mahanadi Basin is a polycyclic, peri-cratonic passive margin basin characterized by NE–SW trending horsts and grabens system. Its tectono-sedimentary evolution (figure 1) reflects initial Gondwana rifting, followed by passive margin development and Miocene-to-present deltaic progradation (source: report on Mahanadi Basin by DGH, India). Mahanadi river was the major contributor of sediments throughout the Paleogene and Early Miocene. After mid-Miocene, the sediments input has been from both Mahanadi as well as Ganga River systems. The stratigraphic sequence comprises rift-phase clastic, deep-water fan systems, and carbonate intervals which result significant lateral and vertical heterogeneity.

The block under study has a well-established biogenic petroleum system. Key exploration targets include Mio-Pliocene Channel-Levee Complexes (CLC), which have demonstrated significant gas accumulations. Eocene and Oligocene sequences also show encouraging leads. However, the complex CLC sediment geometry and abrupt velocity transitions often hinder accurate depth imaging and reservoir delineation in CLCs. Also, the strati-structural complexities pose a challenge for seismic velocity model building, especially for imaging deeper and geologically intricate zones. Our FWI velocity modelling work addresses these challenges by producing high-resolution, geologically consistent velocity models that resolve subtle velocity variations within and around CLC systems to foster exploration derive.

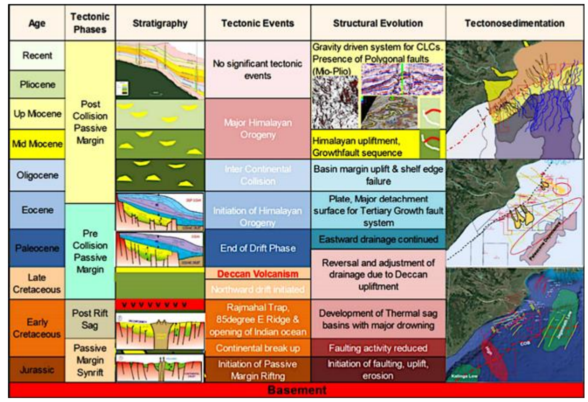

Figure 1: Techno-sedimentary evolution of Mahanadi Basin

Broadband Seismic Data Details

The FWI study is carried out using a recently acquired 3D broadband slant streamer data. The detailed acquisition parameters are provided in table 1. The narrow azimuthal coverage and low xline to inline offset distribution is evident form figure 2. Two sources were used, each towed 50 m apart and fired in a flip -flop pattern. This is a deep-water acquisition with water depths ranged between 450 m and 1500 m. the representative shot in figure 3 shows that direct arrival is distinct, the wavefield mostly reflection dominated, refraction/diving waves are observed mostly in the far offset.

Parameter	Value
Streamer	10 Slant: 8-30m
Bin size	6.25mX25m
Nominal fold	80
Maximum offset	8000m
Source interval	50m Flip-Flop
Receiver interval	12.5m
No. of Channels	6480 (10x648)

Table 1: Broadband seismic survey parameters

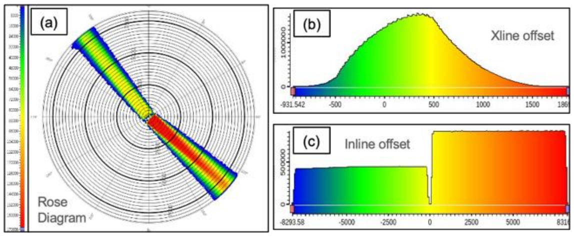

Figure 2: (a) Offset azimuth rose-diagram, (b) Xline offset and (c) Inline offset distribution of the used seismic data

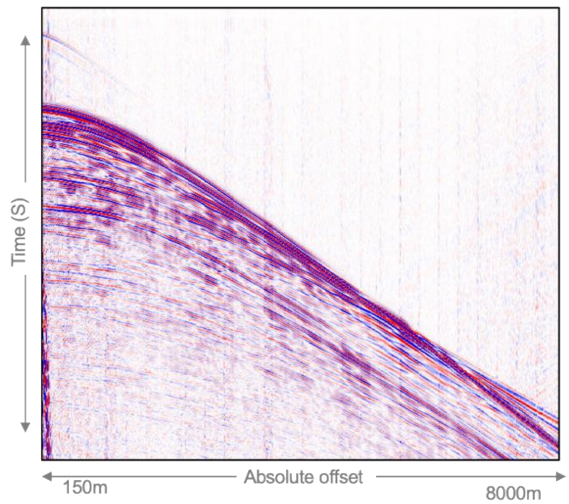

Figure 3: Single receiver line of a representative raw shat gather. A zero-phase bandpass filter (1.5 Hz, 24 dB/octave – 25Hz, 48 dB/octave) has been applied to to attenuate swell noise and enhance the wavefields.

In order to identify the optimal low-frequency content available in the data and best suitable for inversion, spatial phase plots (Figure 4) were analysed. The raw shot gathers were Fourier transformed trace-by-trace, and phase values at individual frequencies were mapped to the corresponding receiver positions. Coherent spatial structures in these phase plots indicate the presence of source-generated signals (Warner et al., 2013). Strong signal-to-noise ratio (S/N) is evident at 4.5 Hz, 4.0 Hz and 3.5 Hz, as appeared by concentric ring-like features cantered around the source. At 3.0 Hz although the data is noisier, the source signature remains clearly identifiable. However, at 2.5 Hz, the S/N degrades significantly. Based on this analysis, 3.0 Hz is considered the reliable low-frequency limit for initiating inversion on this dataset.

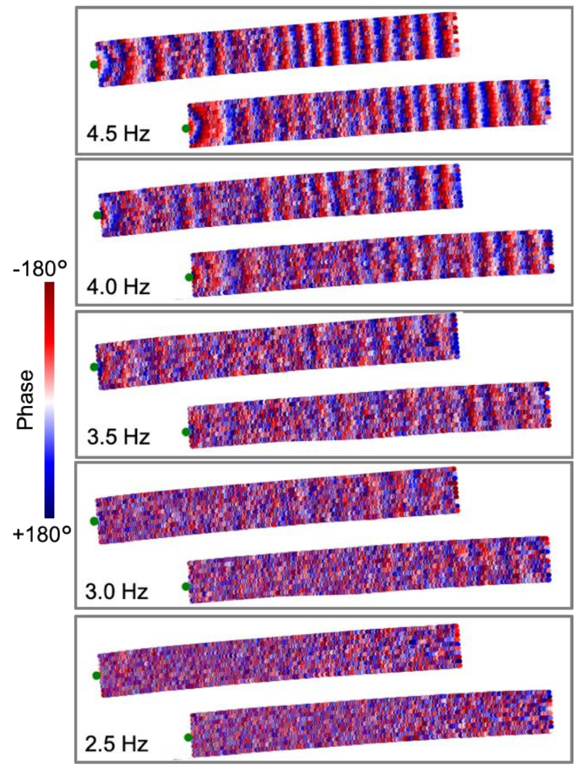

Figure 4: Spatial phase variation as a function of frequency for two representative shot gathers, illustrating lateral wavefield coherence and phase behaviour across the spread

The AWI-RWI-LSFWI Framework

The foundation of AWI-RWI-FWI based velocity modeling approach was first proposed by Warner et al., 2016. It a multi cost function based global optimization workflow. It utilizes time-domain wavefield modelling and gradient-based optimization. Below are the key aspects of the inversion schemes as proposed:

<u>AWI (Adaptive Waveform Inversion):</u> AWI principally matches the kinematics of the wavefield. AWI minimizes cycle-skipping by matching seismic traces of observed and modelled data, trace-by-trace using convolutional filters rather than point-by-point amplitude

differences. This convolutional filter then pushes to a zero-lag, unit-amplitude, delta function. It has enhanced sensitivity to reflection moveout, and reduced sensitivity to amplitude mismatches, especially those produced by unmodelled attenuation and elastic phenomena.

RWI (Reflection Waveform Inversion): derives macro-model updates by leveraging subtle kinematic differences in pre- and post-critical reflections. It is particularly effective in updating long-wavelength velocity structures using reflection data, even in the absence of low-frequency signal components. RWI is a sort of tomography implementation within FWI framework but the key difference is RWI takes place with surface-multiples, interbed multiples and surface ghosts all retained within the input data. These are modelled during inversion, and the multiples as well as the primary reflections contribute to the macro-velocity updates.

LS-FWI (Least square FWI): The low-wavenumber kinematic background, or macro model, is first progressively refined using AWI-RWI. It ensures robustness against cycle-skipping and improved data fit. This refined background model then provides a stable and geologically consistent foundation for subsequent inversion stages. Building on this, LS-FWI employs full wave-equation modelling and amplitude-sensitive objective functions to resolve high-frequency velocity details with improved fidelity.

Methodology

In our study, the velocity model building was performed using a structured multi-stage workflow combining data preconditioning, model initialization, and progressive full waveform inversion using the AWI-RWI-LSFWI approach. The classical approach as proposed by Warner et al., 2013, 2022 & Shah et al., 2024 is optimized based on geological setup and data specific challenges. Initially, preconditioning of the raw shot gathers was carried out by correcting for recording delays and rejecting spurious traces. An average source wavelet was then estimated using short-offset direct arrivals. This estimated wavelet was validated by comparing modelled and observed direct arrivals to ensure wavelet fidelity. The starting velocity model was generated by converting pre-stack time-domain RMS velocities to interval velocities, followed by a fast long-wavelength tomographic refinement using reflection-based updates. Anisotropic parameters (ε and δ) were derived from well log data and smoothed to generate a geologically consistent VTI background model.

Acoustics anisotropic inversion was performed proceeding from 3 Hz to 12 Hz in a stagged manner. Gardner's relation is used to construct spatially variable estimates of density. At first AWI is used to invert diving waves which build a kinematically accurate near-seafloor and shallow velocity model. Once the diving-wave zone was accurately resolved, RWI was applied to update the deeper macro-model using reflections. Finally alternating AWI and LSFWI iterations were applied to refine the velocity model at fine scale that minimizes amplitude misfit and avoided cycle-skipping. This combined inversion strategy produced a high-fidelity background velocity model with fine-scale resolution. The above methodology is summarized below in the form of key workflow steps:

- Preconditioning and editing of raw shot data
- Average wavelet estimation from short-offset direct arrivals
- Spatial frequency analysis to determine inversion starting frequency
- Preparation of initial smooth velocity model and well derived smooth anisotropic (ε, δ) parameters
- Acoustic VTI full waveform inversion using the AWI-RWI-LSFWI strategy
- AWI-driven inversion of diving waves for shallow velocity updates
- RWI-driven updates to deep macro-model using reflected arrivals

- AWI–LSFWI for amplitude-based high-resolution velocity refinement
- Common image gather analysis for model validation and quality control

Results

The AWI stage effectively reconstructed the broad velocity trends, minimizing kinematic misfits. This enhancement in image fidelity allowed better delineation of major stratigraphic boundaries. RWI further refined the background velocity, particularly at deeper stratigraphic levels which resulted improve flatness of seismic events.

In figure 5, the interleaved display of field and modelled data confirms a good trace match in both kinematics and amplitudes. This ensures the reliability of the inverted model. The final velocity model reveals sharp velocity contrasts with improved lateral continuity, especially across the Channel-Levee-Complexes (CLCs) within the Miocene–Pliocene sequences. Zones of low velocity within the channels are consistent with gas-charged sediment fill and are highlighted in figure 6. These features were absent in the initial velocity model and represents the improvement brought by the inversion. A similar low-velocity channel is also visible in the depth slice of figure 7, supporting the presence of a multi-channel system. These channels have significant exploration potential, and the localized velocity drop enhances confidence in hydrocarbon presence.

In the Oligocene-Miocene section, the final model (see figure 8) reveals localized high-velocity anomalies. These are interpreted as compacted clastic units, supported by their strong RMS amplitude response. Though they resemble channel features in amplitude and frequency content, their distinct velocity signature allows effective separation, aiding in prospect de-risking.

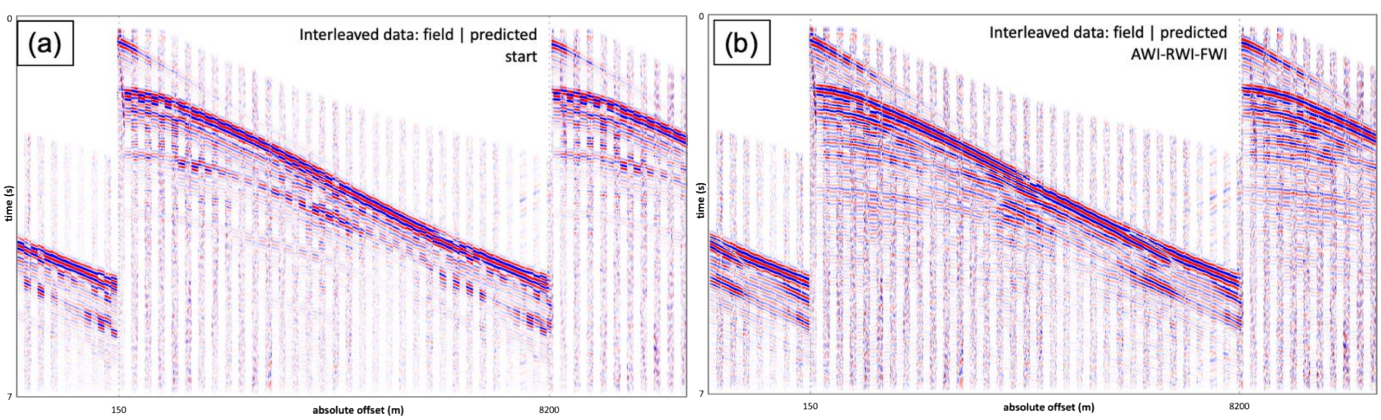

Figure 5: Interleaved shot gather showing field data alongside predicted data using (a) the initial velocity model and (b) the final inverted velocity model. Improved trace alignment and amplitude match in (b) highlight the effectiveness of the inversion process.

High-Resolution Velocity Model Building Using Full Waveform Inversion: A Case Study from Deep-Water Block Mahanadi Basin, India

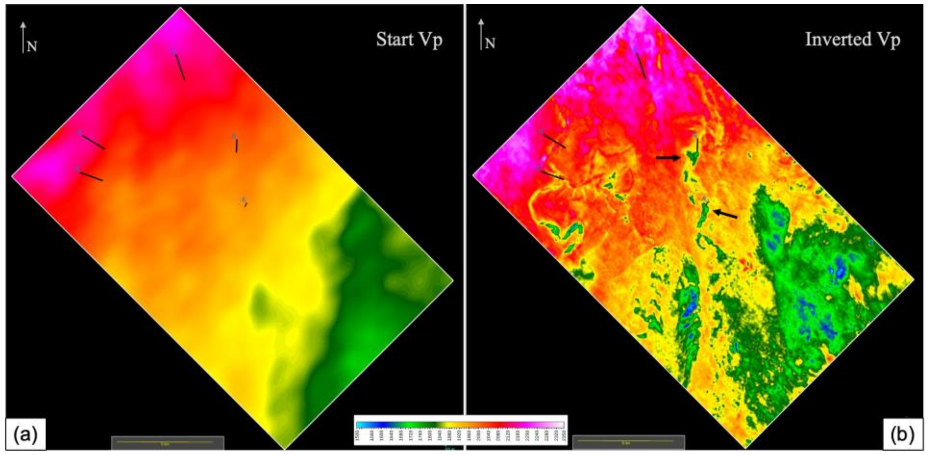

Figure 6: Depth slice at 1750 m showing (a) the starting velocity model and (b) the inverted velocity model. The inversion successfully resolves a low-velocity gas-bearing channel feature, already explored.

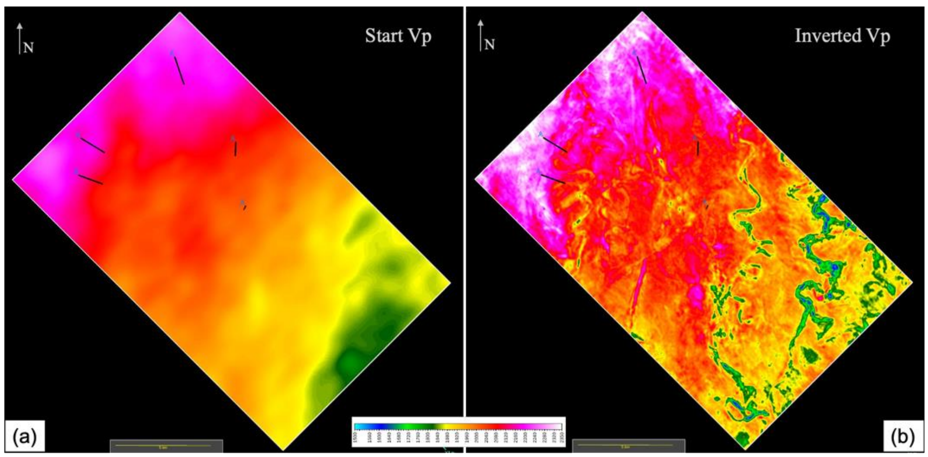

Figure 7: Depth slice at 1900 m showing (a) the starting velocity model and (b) the inverted velocity model. The inversion clearly delineates Channel-Levee Complexes (CLCs), with localized velocity drops

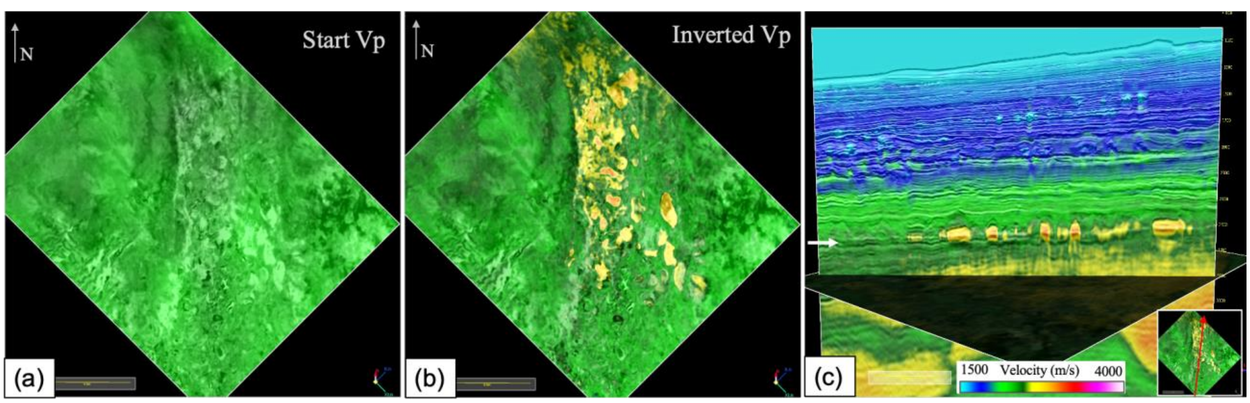

Figure 8: Velocity variation within Oligocene-Miocene sequence: (a) start velocity slice on stack, (b) inverted velocity slice on stack at 2550m and (b) arbitrary section, depicting sharp velocity contrast within clastic, highlighting subtle heterogeneities.

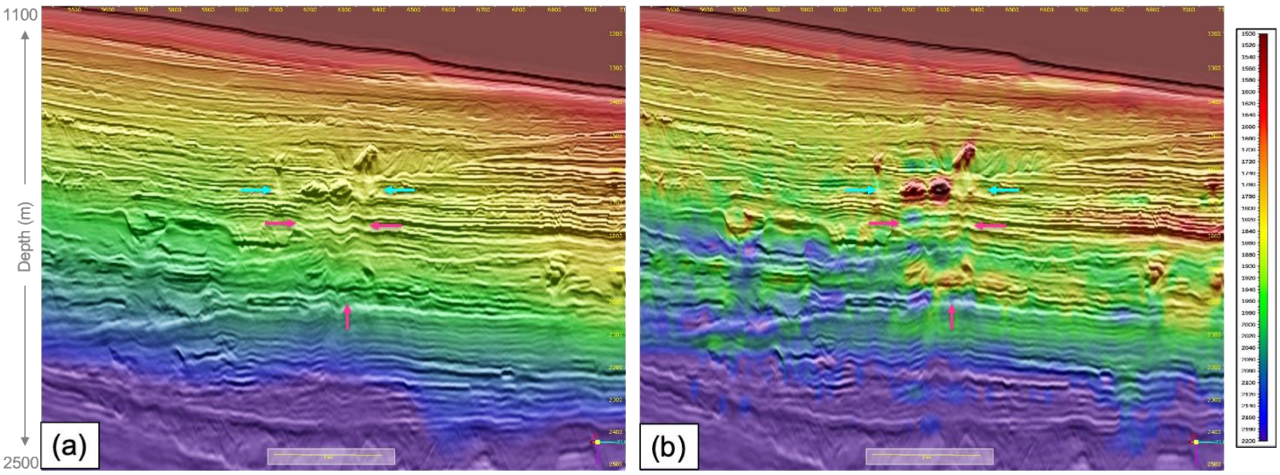

Figure 9: Resolves depth structural sag artifacts by delineation of a low-velocity channel. Migrated depth stacks are overlaid on associated (a) the initial velocity model and (b) the inverted velocity model. The inversion successfully flattens the structural sags by incorporating realistic low-velocity anomalies, leading to improved structural positioning and imaging accuracy.

An important benefit of capturing the true velocity structure is seen in figure 9. The structural sags caused by unresolved low-velocity anomalies in tomography are corrected. The improved velocity model realigns deeper Miocene reflectors, reducing structural uncertainties and enhancing depth accuracy.

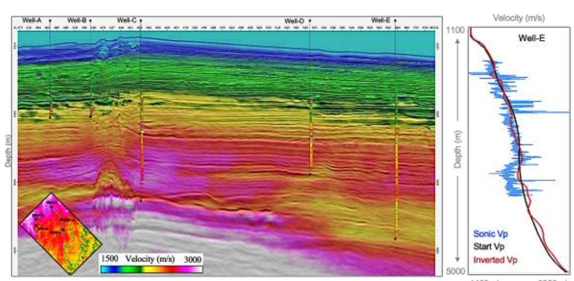

Figure 10: The inverted velocity model is in prominent agreement with well velocity trend. Inverted velocity at the deepest well shows improved match.

The arbitrary line section in figure 10 passing through drilled wells shows strong conformity between the final model and well log velocities. Furthermore, the final model flattens the common image gathers (as illustrated in figure 11). The flattened common image gathers confirm the robustness of the migration velocity model and ensure imaging accuracy.

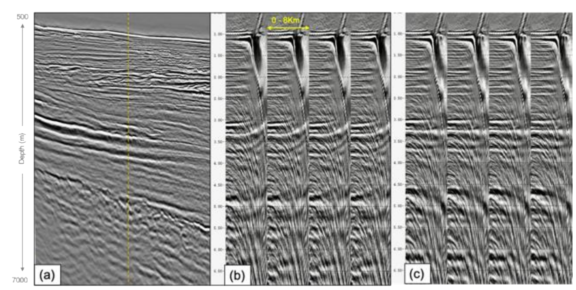

Figure 11: (a) Reference depth stack with common image offset gathers with (b) start velocity model and (c) final inverted velocity model.

Conclusion

This study demonstrates the effectiveness of the multi-stage AWI-RWI-LSFWI inversion workflow in generating a high-resolution velocity model for a complex deep-water setting using narrow-azimuth streamer data having reliable start frequency 3.0 Hz. The final outputs successfully resolve channel-levee complexes, reduces structural artifacts and produce flatten image gather. The workflow is computationally efficient due to the progressive inversion strategy. Its multi-stage structure allows easy adaptation to different geological settings and data types. This makes the methodology highly applicable to a wide range of complex exploration challenges.

References

Mahanadi Basin Geology, source DGH, India

Warner, M. et al. (2013), Anisotropic 3D full-waveform inversion, Geophysics, VOL. 78, R59–R80

Guasch, L., Warner, M., Stekl, I., & Umpleby, A. (2016). Adaptive waveform inversion: Theory. Geophysics, 81(6), R429–R445.

Warner, M. et al. (2022). Full-waveform inversion in complex settings: Applications and field case studies. The Leading Edge.

Shah N. et al., (2024) FWI imaging through basalt, EAGE Annual 85th Conference & Exhibition, Oslo, Norway.

Acknowledgements

The authors are thankful to Director (Exploration), ONGC for providing the opportunity to carry out this project. The team is also thankful to COI-GEOPIC, Head Processing GEOPIC and Head-INTEG GEOPIC for their valuable suggestions and for providing resources to carry out this work. The authors would like to thank ONGC for giving permission to publish the work.

The view expressed in this paper are solely of the authors.